

**Structural basis for differences in dynamics induced by Leu versus Ile residues
in the CD loop of Kir channels**

Shouqin Lü^{1,2,3,ξ}, Hailong An^{4,ξ}, Hailin Zhang^{5,*}, Mian Long^{1,2,3,*}

¹Center of Biomechanics and Bioengineering, ²Key Laboratory of Microgravity (National Microgravity Laboratory) and ³Beijing Key Laboratory of Engineered Construction and Mechanobiology, Institute of Mechanics, Chinese Academy of Sciences, Beijing 100190, China. ⁴

Key Laboratory of Molecular Biophysics, Hebei Province, Institute of Biophysics, School of Sciences, Hebei University of Technology, Tianjin 300401, China. ⁵Key Laboratory of Neural and Vascular Biology, Ministry of Education, The Key Laboratory of Pharmacology and Toxicology for New Drug, Hebei Province, Department of Pharmacology, Hebei Medical University, Shijiazhuang 050017, China.

^ξShouqin Lü and Hailong An contributed equally to this work.

*Address correspondence to:

Dr. Hailin Zhang, Tel. 86-311-86265562, Fax. 86-311-86265562, zhanghl@hebmu.edu.cn, Hebei Medical University, Shijiazhuang 050017, China, or Dr. Mian Long, Tel. 86-10-82544131, Fax. 86-10-82544131, mlong@imech.ac.cn, Institute of Mechanics, Chinese Academy of Sciences, Beijing 100190, China.

Supplementary material

ESM_1: Schematic of definitions for R78-R186 distance, TMD-CTD distance, and sidechain orientations of Ile and Leu residues.

ESM_2: Sequence alignments of the CD loop for human and mouse Kir channels.

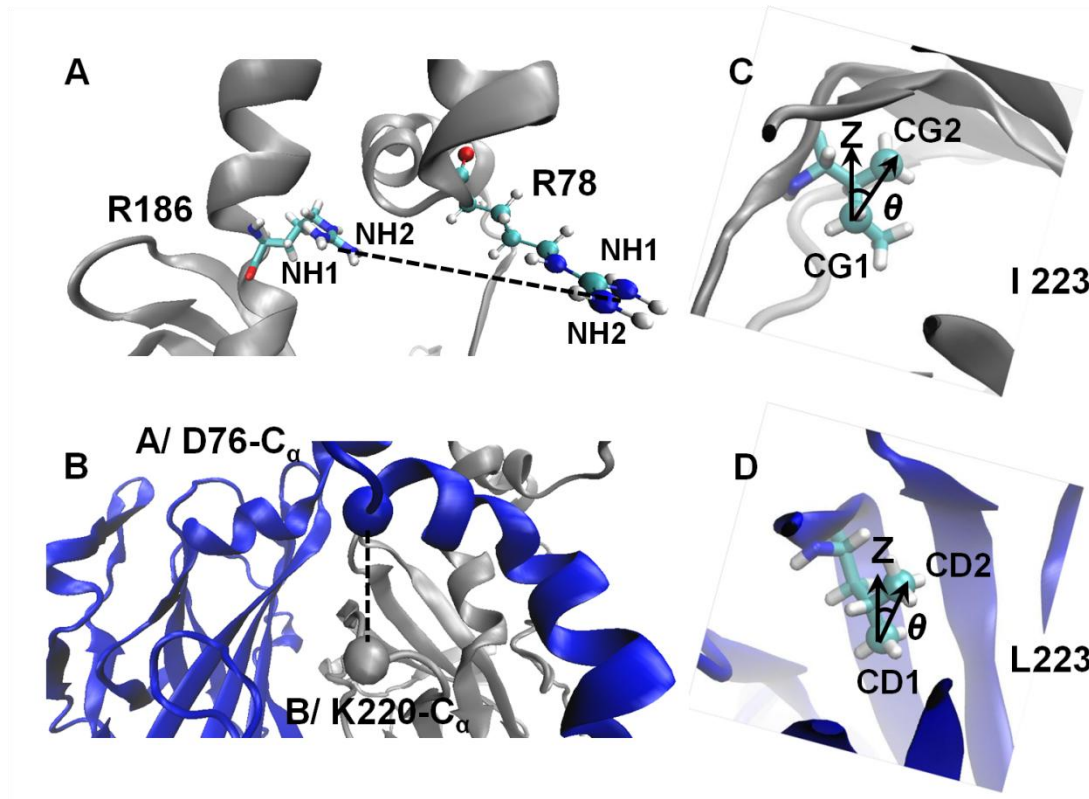
ESM_3: Global Hbond interactions and the distributions among binding sites for PIP₂-liganded chicken Kir2.2 systems

ESM_4: Evolution of R186-R78 distance for PIP₂-liganded chicken Kir2.2 systems.

ESM_5: Evolution of TMD-CTD distance for PIP₂-liganded chicken Kir2.2 systems.

ESM_6: Conformational stability of PIP₂-absent chicken Kir2.2 WT and I223L mutant systems

ESM_1



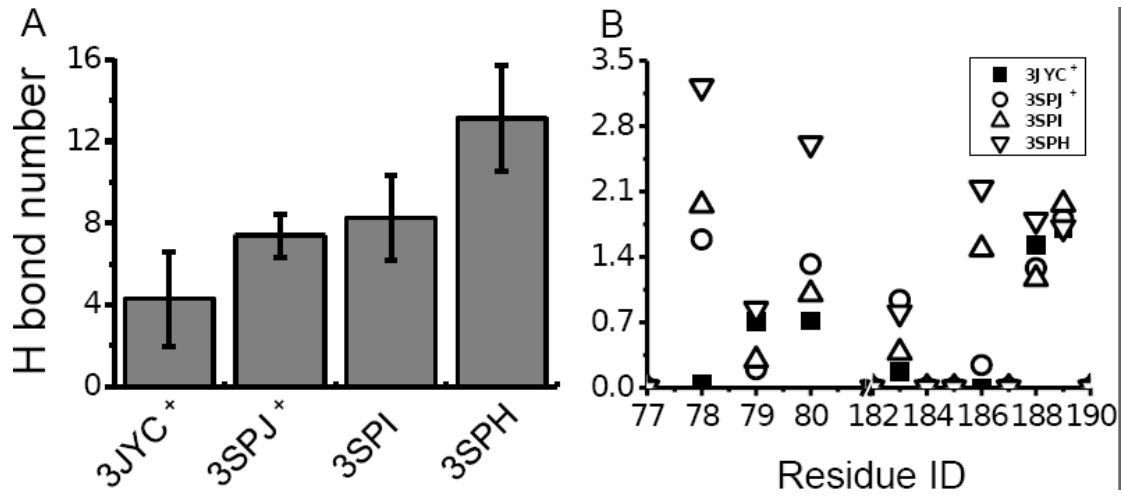
ESM_1: Schematic of definitions for R78-R186 distance (A), TMD-CTD distance (B), and sidechain orientations of I223 (C) and L223 (D) residues.

ESM_2

A	Human KIR1.1	217	R K S L L I G S H I Y	227
	Human KIR2.1	218	R K S H L V E A H V R	228
	Human KIR2.2	219	R K S H I V E A H V R	229
	Human KIR2.3	210	R K S H I V E A H V R	220
	Human KIR2.4	223	R R S H L V E A H V R	233
	Human KIR3.1	219	R N S H M V S A Q I R	229
	Human KIR3.2	228	R N S H I V E A S I R	238
	Human KIR3.3	196	R S S H I V E A S I R	206
	Human KIR3.4	225	R N S H I V E A S I R	235
	Human KIR4.1	204	R K S L L I G C Q V T	214
	Human KIR4.2	203	R K S L L I Q C Q L S	213
	Human KIR5.1	207	R P N H V V E G T V R	217
	Human KIR6.1	216	R K S M I I S A S V R	226
	Human KIR6.2	206	R K S M I I S A T I H	216
	Human KIR7.1	195	R P S P L T S V R V S	205
B	Mouse KIR1.1	218	R K S L L I G S H I Y	228
	Mouse KIR2.1	218	R K S H L V E A H V R	228
	Mouse KIR2.2	219	R K S H I V E A H V R	229
	Mouse KIR2.3	209	R K S H I V E A H V R	219
	Mouse KIR2.4	223	R R S H L V E A H V R	233
	Mouse KIR3.1	219	R N S H M V S A Q I R	229
	Mouse KIR3.2	230	R N S H I V E A S I R	240
	Mouse KIR3.3	196	R S S H I V E A S I R	206
	Mouse KIR3.4	225	R N S H I V E A S I R	235
	Mouse KIR4.1	204	R K S L L I G C Q V T	214
	Mouse KIR4.2	230	R K S L L I Q C Q L S	240
	Mouse KIR5.1	207	R P N H V V E G T V R	217
	Mouse KIR6.1	216	R K S M I I S A S V R	226
	Mouse KIR6.2	206	R K S M I I S A T I H	216
	Mouse KIR7.1	195	R P S P L T N V R V S	205
Chicken Kir2.2	219	R K S H I V E A H V R	229	

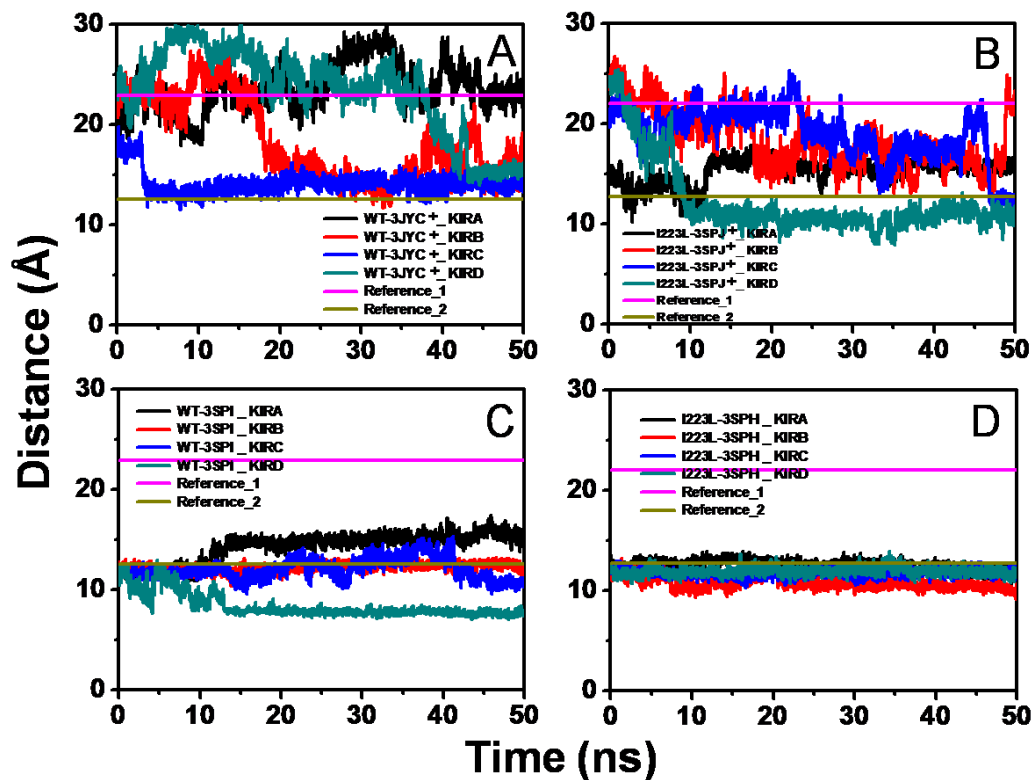
ESM_2: Sequence alignments of the CD loop for human (A) and mouse (B) Kir channels. The chicken Kir2.2 sequence was also aligned with the mouse Kir channels, and the residue that was focused in this study was marked in yellow.

ESM_3



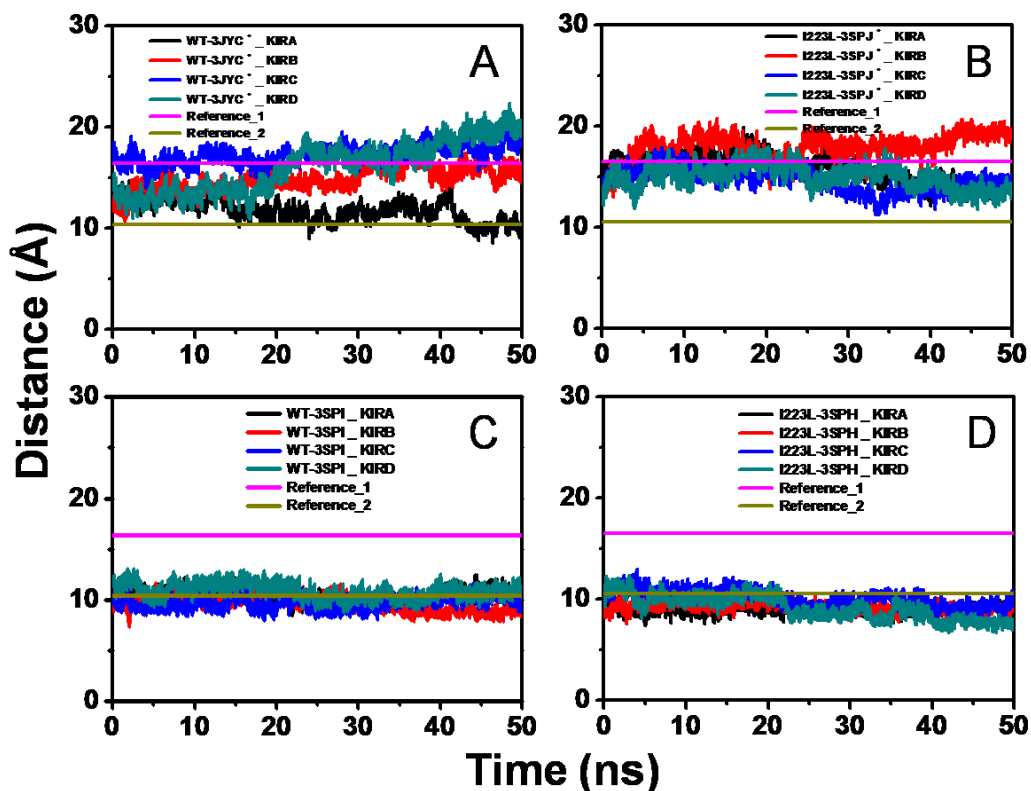
ESM_3: Global H bond interactions (A) and the distributions among binding sites (B) for PIP₂-liganded chicken Kir2.2 systems. The data was presented as mean \pm SD (A) or mean only (B) of tetramer after the last 10-ns trajectory average of each subunit.

ESM_4



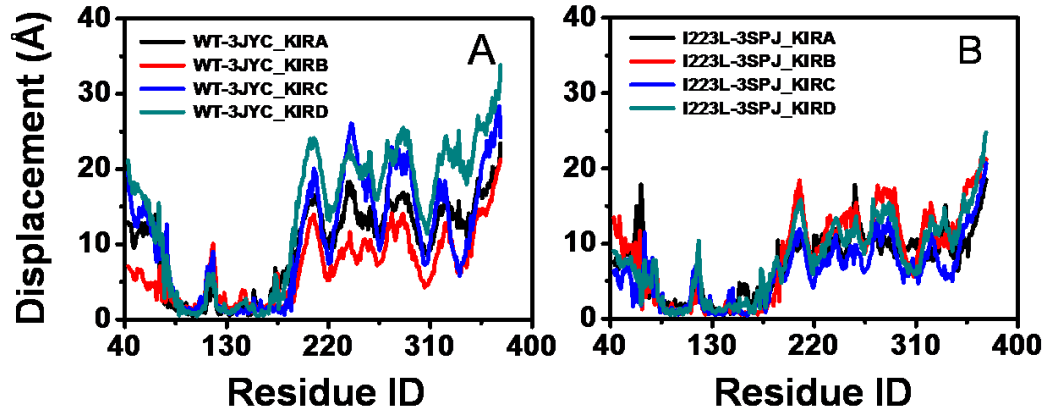
ESM_4: Evolution of R186-R78 distance for PIP₂-liganded chicken Kir2.2 systems. The evolution along 50-ns equilibration of each subunit was presented for artificially PIP₂-added WT (A) and I223L mutant (B) systems, as well as PIP₂ co-crystallized WT (C) and I223L mutant (D) systems. The references 1 and 2 were the corresponding R78-R186 distances of crystallized PIP₂-absent (reference_1) and PIP₂-presence (reference_2) WT and I223L mutant structures.

ESM_5



ESM_5: Evolution of TMD-CTD distance for PIP₂-liganded chicken Kir2.2 systems. The evolution along 50-ns equilibration of each subunit was presented for artificially PIP₂-added WT (A) and I223L mutant (B) systems, as well as PIP₂ co-crystallized WT (C) and I223L mutant (D) systems. The references 1 and 2 were the corresponding TMD-CTD distances of crystallized PIP₂-absent (reference_1) and PIP₂-presence (reference_2) WT and I223L mutant structures.

ESM_6



ESM_6: Conformational stability of PIP₂-absent chicken Kir2.2 WT (A) and I223L mutant (B) systems. The displacement for each residue was defined as the distance between the heavy atom center of equilibrated snapshot and that of the initial crystallized structure upon the alignment of the backbone atoms of transmembrane M1 (L85-A105) and M2 (C155-I180) helices, and the data were shown as the average of last 10-*ns* equilibration.